of identical chemical composition, doped with rare-earth activators, may be extended to many other hosts as well, provided, of course, that the glassy counterpart of the crystalline material can be successfully prepared in homogeneous pieces of sufficient size.

The use of rare-earth fluorescence as a probe under these circumstances simplifies the analysis of data considerably, particularly if it is done on a comparative basis, and offers the following advantages: First, various processes involved in luminescence such as energy transfer and quenching, occurring in these materials, can be better understood. Second, it is possible to investigate certain fundamental differences between the crystalline state characterized by its long-range order and the amorphous glassy state characterized by short-range order only. The annealing of glass samples while emission is monitored at various stages in the recrystallization cycle is one possible technique. Our preliminary results suggest that further quantitative studies along these general lines should prove to be fruitful.

*Present address: Electrical Engineering Dept., McGill University, Montreal 110, P. Q., Canada.

[1]G. O. Karapetyan and A. L. Reishakrit, Izv. Akad. Nauk SSSR Neorgan. Materialy 3, 217 (1967).

[2]E. Snitzer, Proc. IEEE 54, 1249 (1966).

[3]Z. J. Kiss and R. J. Pressley, Proc. IEEE 54, 1236 (1966).

[4]A. Linz, V. Belruss, and C. S. Naiman, J. Electrochem. Soc. 112, 60C (1965).

[5]Mohan Munasinghe, S. M. and E. E. thesis (MIT, 1969) unpublished).

[6]Atomic fraction $= N_a / (N_a + N_h) \approx N_a/N_h$, when $N_h \gg N_a$ and where N_a is the density of Nd^{3+} activator ions; N_h is the density of Ba^{2+} host matrix cation which is replaced by activator ions.

[7]C. Hirayama, Phys. Chem. Glasses 7, 52 (1966).

[8]L. G. Van Uitert, *Luminescence of Inorganic Solids* (Academic, New York, 1966), p. 484.

[9]D. W. Harper, Phys. Chem. Glasses 5, 11 (1964).

[10]G. E. Peterson and P. M. Bridenbaugh, J. Opt. Soc. Am. 54, 644 (1964).

[11]Yu. K. Voronko and V. V. Osika, Zh. Eksperim. i Teor. Fiz. Pis'ma v Redaktsiyu 5, 357 (1967) [Sov. Phys. JETP Letters 5, 295 (1967)].

[12]M. J. Weber, *Physics of Quantum Electronics* (McGraw-Hill, New York, 1966), p. 350.

[13]D. L. Dexter, J. Chem. Phys. 21, 836 (1953).

[14]D. L. Dexter and J. H. Schulman, J. Chem. Phys. 22, 1063 (1954).

[15]J. D. Axe and P. F. Weller, J. Chem. Phys. 40, 3066 (1964).

[16]L. G. Van Uitert and L. F. Johnson, J. Chem. Phys. 44, 3514 (1966).

[17]R. J. Birgenau, Appl. Phys. Letters 13, 193 (1968).

Electron Spin Resonance of Mn^{2+} in CaF_2[†]

R. J. Richardson, Sook Lee,* and T. J. Menne
*McDonnell Douglas Research Laboratories, McDonnell Douglas Corporation,
St. Louis, Missouri 63166*
(Received 12 July 1971)

A critical investigation has been made of the room-temperature electron-spin-resonance (ESR) spectra of $^{55}Mn^{2+}$ present in dilute concentrations in CaF_2, and a detailed quantitative explanation of this ESR center was obtained. As a result, several uncertainties associated with the previous interpretation of this center have been resolved. The theoretical spectra which fit the experimental data were obtained from a spin Hamiltonian characterized by the cubic crystal-field parameter $a = 0 \pm 0.1$ G, the manganese hyperfine constant $A = -100.8 \pm 0.1$ G, the fluorine superhyperfine constants $T_{\parallel} = +15.3 \pm 0.1$ G and $T_{\perp} = +6.3 \pm 0.1$ G, and $g = 2.0010 \pm 0.0005$.

I. INTRODUCTION

The experimental electron-spin-resonance (ESR) spectra of Mn^{2+} substituted for the divalent cation in fluorite-type crystals exhibit six allowed ^{55}Mn ($I = \frac{5}{2}$) hyperfine lines. In crystals containing very dilute amounts of Mn^{2+}, each of these hyperfine lines is split further into a complicated superhyper-

fine structure arising from the ligand[19] F $(I = \frac{1}{2})$ nuclei.[1-7] Substantial efforts have been devoted to explaining the observed ESR structure in terms of the second-order ^{55}Mn hyperfine effect, a small amount of cubic crystal-field splitting of the ground state $(^{6}S_{5/2})$ of the ion, and the superhyperfine interaction with the nearest-neighbor (nn)^{19}F nuclei.[1,2,6,7] To our knowledge, however, the experimental spectra have never been critically analyzed in a quantitative manner because of the complexity introduced in the theoretical ESR spectra by the various effects mentioned above. Thus, there has always been some doubt as to the accuracy of our present understanding of the widely studied Mn^{2+} center in the alkaline-earth fluoride lattice.

We have recently undertaken a careful investigation of this problem, initially in CaF$_2$: Mn^{2+}, and the results are reported in this paper. We have been successful in accurately explaining the experimental ESR data, removing ambiguities associated with previous investigations, and providing a better understanding of the Mn^{2+} center in alkaline-earth flouride crystals.

II. EXPERIMENT

Three samples of single-crystalline CaF$_2$ containing, respectively, nominal 10^{-4}, 10^{-2}, and 1 wt% Mn^{2+} concentrations were obtained from Optovac, Inc. The ESR investigations were made with two different Varian 4500 spectrometers: an X-band spectrometer operating at a microwave frequency in the vicinity of 9 GHz, and a K_a-band spectrometer operating near 35 GHz. Both of the spectrometer systems employed a 100-kHz field-modulated detection unit and a 12-in. rotatable electromagnet equipped with a field-regulated power supply. The primary purpose of the K_a-band ESR investigation was to check the results of our analysis of the X-band ESR data for a different value of the microwave frequency and for a different range of static field values. Unless specifically mentioned, the ESR data reported in this work were taken with the X-band spectrometer at room temperature.

The frequency of the klystron was measured by observing harmonic beats of the microwave frequency with the output of a Hewlett-Packard 540B transfer oscillator and by measuring the frequency of the transfer oscillator with a Hewlett-Packard Model 5245L electronic counter equipped with a 5253B frequency converter. In this way the frequency can be determined to an accuracy greater than 1 part in 10^6. This same electronic counter was used to measure the frequency of a proton NMR gaussmeter that monitored the magnetic field strength.

Figures 1–3 show the ESR spectra obtained from the crystal with the 10^{-4} wt% ion content for the

three crystal axes [100], [110], and [111] parallel to the external magnetic field $\vec{H}$. The crystal was critically aligned by monitoring the intensity of the superhyperfine structure. Since a turns out to be zero and since g and A are independent of angle, the narrowest and hence most intense lines occur when the number of angles that the magnetic field makes with the individual fluorines is as degenerate as possible (see Sec. III). Changes in the intensity of the observed resonance lines are noticeable for differences in angle of 2 or 3 tenths of a degree.

The details of the complicated superhyperfine structure changed (particularly for the $m = \pm \frac{5}{2}$ ^{55}Mn components) when the microwave frequency was changed by only 0.5 GHz. The ESR spectra obtained at the K_a-band frequency exhibited fluorine superhyperfine structure completely different from the X-band spectra.

An investigation was conducted to check the possibility that some of the resonance lines in the experimental spectra might arise from other accidental paramagnetic impurities such as Eu^{2+} and Gd^{3+} which are commonly found in CaF$_2$ and which yield ESR spectra readily observable at room temperature in the magnetic field range for the Mn^{2+} spectra.[8] If the sample contained these impurity ions, some of their fine-structure component lines would appear on both the low- and high-field sides of the Mn^{2+} ESR spectrum for $\vec{H} \parallel$ [100]. However, a carefule search from 0 to 10 kG revealed no other resonances lines.

The ESR spectra observed in the CaF$_2$ sample containing the 10^{-2} wt% Mn^{2+} concentration exhibited hyperfine and superhyperfine structures similar to those obtained from the sample with the lower concentration of Mn^{2+}. However, the spectra showed an increased line-broadening effect, and some of the superhyperfine lines displayed in Figs. 1–3 were not resolved in this sample.

The sample containing 1 wt% Mn^{2+} displayed ESR spectra which exhibited six rather broad ^{55}Mn hyperfine component lines without any resolved fluorine superhyperfine structure. These spectra were independent of the crystal orientation with respect to the magnetic field direction within experimental error.

To determine the absolute sign of the hyperfine coupling constant A for Mn^{2+} in CaF$_2$, the low-temperature behavior of the hyperfine splitting of the spectrum from the sample containing 1 wt% Mn^{2+} was investigated in an experiment similar to that performed previously in this laboratory[9] for SrF$_2$: Mn^{2+}. As was noted for SrF$_2$, the separation between the outermost ^{55}Mn hyperfine lines was observed to increase as the temperature was lowered below 4.2 K, showing that the sign of A is unambiguously negative.
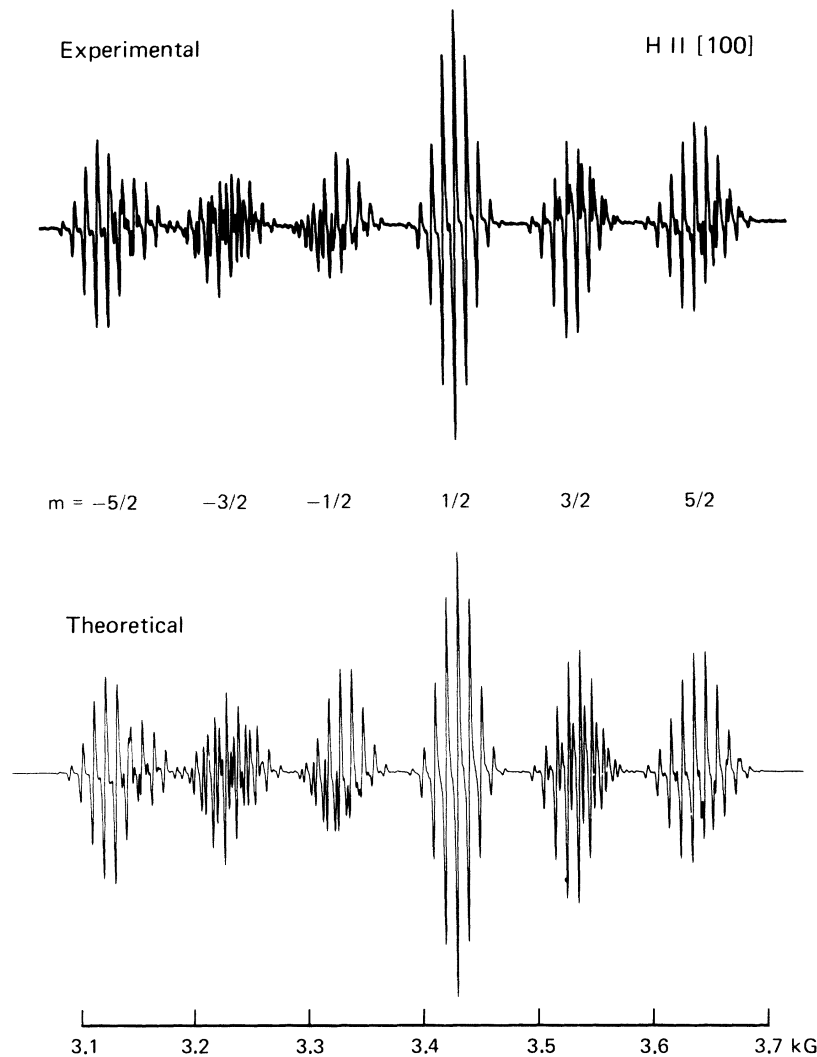
FIG. 1. Experimental and theoretical ESR spectra for Mn^{2+} in CaF_2 with $\vec{H} \parallel [100]$ at 9.51 GHz.

III. THEORETICAL

Manganese is normally substitutionally incorporated into the alkaline-earth fluoride lattice at a cation cubic site surrounded by eight nn fluoride ions which are situated at the corners of a simple cube. The ESR spectrum observed for this complex can be described by the spin Hamiltonian

$$\mathcal{H} = g\,\mu_B\,\vec{H}\cdot\vec{S} + \tfrac{1}{6}\,a\,[S_x^4 + S_y^4 + S_z^4 - \tfrac{1}{5}\,S(S+1)\,(3S^2 + 3S - 1)]$$

$$+ A\,\vec{S}\cdot\vec{I} + \sum_{i=1}^{8}\,(\vec{S}\cdot\vec{\overline{T}}_i\cdot\vec{K}_i + {}^{19}\gamma\,\vec{H}\cdot\vec{K}_i)\ . \tag{1}$$

In this expression the first two terms represent the effects of the Zeeman and cubic field splitting of the $^6S_{5/2}$ electronic ground state. The third term is the isotropic hyperfine interaction between the electronic and nuclear spins of $^{55}Mn^{2+}$. The super-

hyperfine interaction of the manganese ion with the eight surrounding fluorines ($K_i = \frac{1}{2}$) and their Zeeman interactions are denoted by the summation of terms with $\overline{\overline{T}}_i$ and $^{19}\gamma$, respectively.

Several investigators have performed perturbation calculations to determine the effects of the various terms using the Zeeman eigenstates as basis states. Materrese and Kikuchi[10] have calculated the cubic field splitting of the $^6S_{5/2}$ ground state. The expression for the magnetic field positions of the transitions characterized by $M - 1 \rightarrow M$ (where M is the electronic magnetic quantum number) is given by

$$H = H_0 - (\tfrac{1}{64}\,a)\,(35\cos^4\theta - 30\cos^2\theta + 3 + 5\sin^4\theta\,\cos4\psi)$$

$$\times (56M^3 - 84M^2 - 134M + 81)\ , \tag{2}$$

where $H_0 = h\nu/g\,\mu_B$, and the coordinate system defined by the Zeeman interaction (i.e., $\vec{H} \parallel z$ axis)
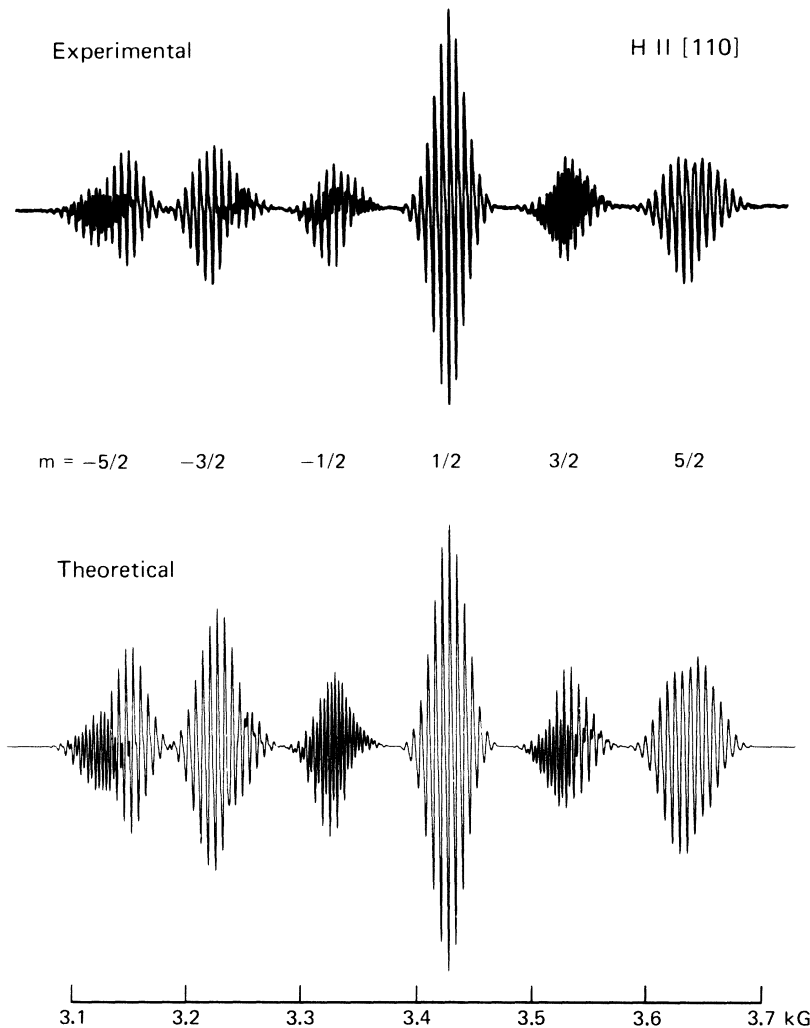
FIG. 2. Experimental and theoretical ESR spectra for Mn^{2+} in CaF_2 with $\vec{H} \| [110]$ at 9.51 GHz.

has the Euler angles (θ, ψ, ϕ) with respect to the cubic field coordinate system.

The effects of the hyperfine interaction have been calculated to second order by Bleaney[11] and to third order by Lacroix.[8] For an isotropic hyperfine interaction, the result for the transitions characterized by $M - 1 \to M$ and $m \to m$ (where m is the nuclear magnetic quantum number) is to add to Eq. (2) the following expression:

$$-Am - (A^2/2H)[I(I+1) - m^2 + m(2M - 1)]$$

$$- (A^3/2H^2)\{(2M - 1)[2I(I+1) - 3m^2]$$

$$- m[S(S+1) + I(I+1) - 2 - m^2] + 3mM(M - 1)\} .$$

$$(3)$$

It should be noted that the expressions for the second- and third-order terms originally given by Bleaney and Lacroix contain $H_0 = h\nu/g\mu_B$; however, H gives a more accurate approximation in an ex-

periment in which the field is swept and the frequency is held constant.

When A is much larger than a, the theoretical ESR spectrum is characterized by six [55]Mn hyperfine lines, each of which is further split into five lines by the higher-order hyperfine effects and/or by the cubic field splitting (a total of 30 lines). The details of each five-line structure depend critically on the relative magnitude of the cubic field splitting and the higher-order hyperfine terms as well as on the value of m. Throughout this paper, we will refer to this five-line structure as fine structure even if only higher-order hyperfine terms are responsible for this splitting.

The interaction of the Mn^{2+} with the eight nn ^{19}F nuclei splits each of the fine-structure lines into numerous superhyperfine lines. When the strength of the nuclear Zeeman interaction is comparable to the superhyperfine interaction, the resultant superhyperfine structure is unusually complicated.
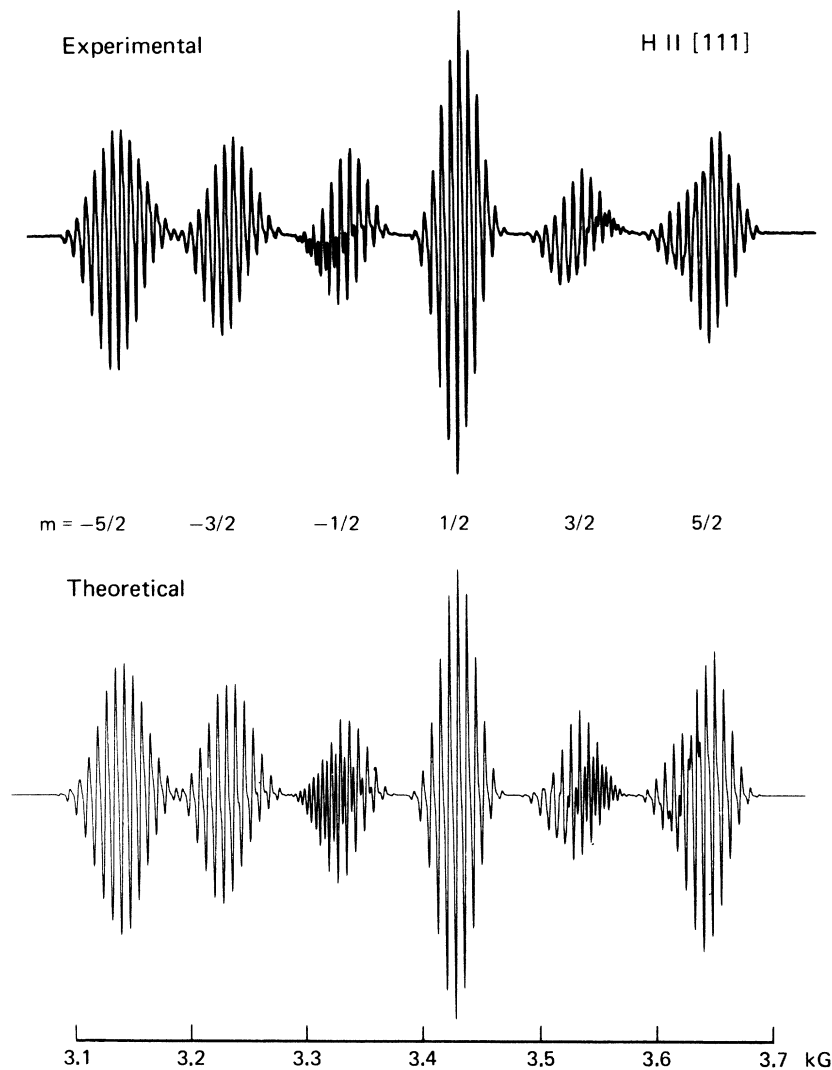
FIG. 3. Experimental and theoretical ESR spectra for Mn^{2+} in CaF$_2$ with $\vec{H}\|[111]$ at 9.51 GHz.

This problem was originally treated in detail by Clogston et al.[12] for Mn^{2+} in ZnF$_2$ and subsequently by Ranon and Hyde[13] for Yb^{3+} in CaF$_2$.

For Mn^{2+} in the alkaline-earth fluorides, the superhyperfine tensor $\overline{\overline{T}}_i$ for the ith fluorine is diagonal in a coordinate system where the z axis is along a body diagonal from the Mn^{2+} to the fluorine. In this coordinate system, the tensor has only two components: $T_\| \equiv T_z$ and $T_\perp \equiv T_x = T_y$. However, in the coordinate system defined by $\vec{H}$ (i. e., $\vec{H}\| z$ axis), the superhyperfine tensor $\overline{\overline{T}}_i$ can be expressed in terms of these two constants ($T_\|$ and $T_\perp$) and α_i, the angle between $\vec{H}$ and the symmetry axis of $\overline{\overline{T}}_i$. In this case it can be shown that the Mth electronic Zeeman energy is perturbed by the amount[13]

$$E_i(M) = k_i \left[P^2(M) \cos^2 \alpha_i + Q^2(M) \sin^2 \alpha_i \right]^{1/2} , \quad (4)$$

where

$$P(M) = MT_\| - {}^{19}\gamma H , \quad Q(M) = MT_\perp - {}^{19}\gamma H . \quad (5)$$

In Eq. (4) k_i is the ith fluorine magnetic quantum number.

Between the eigenstates labeled by the fluorine and electronic magnetic quantum numbers, transitions of the type $\Delta M = -1$, $\Delta k_i = \pm 1$ (normally forbidden) can occur as well as the usually allowed $\Delta M = -1$, $\Delta k_i = 0$ transitions.[14] The $\Delta k_i = \pm 1$ transitions arise because the direction of the effective magnetic field influencing the fluorine nuclei depends significantly on the state of the spin of the manganese ion. This makes it impossible to find a manifold in which the fluorine spins are all diagonal. The relative probabilities for these two types of transitions are given by

$$r_i$$
$$= \frac{1}{2} \left(1 + \frac{P(M)\,P(M-1)\cos^2\alpha_i + Q(M)\,Q(M-1)\sin^2\alpha_i}{E_i'(M)E_i'(M-1)} \right)$$

$$(6)$$

for $\Delta M = -1$, $\Delta k_i = \pm 1$, and

$$s_i$$
$$= \frac{1}{2} \left(1 - \frac{P(M)\,P(M-1)\cos^2\alpha_i + Q(M)\,Q(M-1)\sin^2\alpha_i}{E_i'(M)E_i'(M-1)} \right)$$

$$(7)$$

for $\Delta M = -1$, $\Delta k_i = 0$, where $E_i'(M) = E_i(M)/k_i$. Since there are four transitions for each fluorine, and eight surrounding nn fluorines, there are a total of 4^8 fluorine superhyperfine transitions for each of the 30 resonance lines produced by the hyperfine- and fine-structure interactions.

A simple device for calculating the fluorine line positions and their expected intensities is contained in the expansion of the following expression[12] for arbitrary x:

$$\prod_{i=1}^{8} \left[r_i(x^{U_i} + x^{-U_i}) + s_i(x^{V_i} + x^{-V_i}) \right],$$

$$(8)$$

where

$$U_i = \tfrac{1}{2}\left[E_i(M) + E_i(M-1)\right], \quad V_i = \tfrac{1}{2}\left[E_i(M) - E_i(M-1)\right].$$

$$(9)$$

The exponents of x in this expansion give the field positions of the fluorine superhyperfine transitions, and the associated coefficients give the relative intensities. When computing the expected intensities, it is also necessary to include the proper weight for the relative intensities of the fine-structure lines $(5:8:9:8:5)$.

The calculation of the expected line positions and intensities is greatly simplified when the magnetic field is directed along a crystalline axis with high symmetry. In this case, many of the lines overlap since the fluorines fall into groups with the same α_i. Table I lists the number of fluorines in each group with each value of α_i for $\vec{H}$ parallel to the three major crystallographic directions [100], [110], and [111]. These numbers and angles must be used in the expansion of Eq. (8) to obtain super-hyperfine structure for a given direction. By an examination of Eqs. (4)–(8) it can be seen that the fluorine splitting of the $\alpha = 90°$ spectrum is equal to $T_\perp$ and the splitting of the $\alpha = 0°$ spectrum is equal to $T_{\parallel}$.

IV. ANALYSIS

The first serious attempt to explain the ESR spectra of Mn^{2+} in the alkaline-earth fluoride system was made by Baker, Bleaney, and Hayes[1] in CaF_2. Similar to the ESR data observed in our experiment, their ESR spectra exhibited complicated fluorine superhyperfine structure in addition to the

TABLE I. The number of equivalent fluorines and α_i for $\vec{H}$ parallel to the three major crystallographic axes, where α_i is the angle between $\vec{H}$ and the Ca-F bond direction.

α_i (deg)	$\vec{H} \parallel$ [100]	$\vec{H} \parallel$ [110]	$\vec{H} \parallel$ [111]
0.0	$\cdots$	$\cdots$	2
35.3	$\cdots$	4	$\cdots$
54.7	8	$\cdots$	$\cdots$
70.5	$\cdots$	$\cdots$	3
90.0	$\cdots$	4	$\cdots$
109.5	$\cdots$	$\cdots$	3

six ^{55}Mn hyperfine components. (It appears, however, that their ESR spectra did not reveal all the fine details of the superhyperfine structure observable in Figs. 1–3.)

As in the case of the spectra shown in Figs. 1–3, they noted the striking simplicity of the superhyperfine structure on the fourth ^{55}Mn hyperfine component. This component corresponds to the $m = \tfrac{1}{2}$ transition since we have found A to be negative (see Sec. II). They concluded that the fine structure must be nearly collapsed for this particular hyperfine component, assuming that the crystal field terms of Eq. (2) and the second-order hyperfine term of Eq. (3) are of such magnitude and absolute sign that they almost cancel for $m = \tfrac{1}{2}$. On the basis of this assumption, they calculated that $a = +0.6 \pm 0.4$ G.

In a later paper reporting the investigation of Mn^{2+} in CdF_2, Hall, Hayes, and Williams[2] reconsidered the above analysis and indicated that they were only able to set an upper limit to the magnitude of a for Mn^{2+} in CaF_2 and CdF_2 (i.e., $|a| \leq 4$ G). Subsequent investigators have generally assumed that for Mn^{2+} in the alkaline-earth fluorides, a is some small but nonzero quantity of the order of 1 G. In none of these cases, however, have the experimental ESR data been critically analyzed in detail. Thus, their determinations of the spin-Hamiltonian constants were made solely on the basis of qualitative analyses of the experimental spectra.

The great complexity of the theoretical ESR spectra expected from the spin Hamiltonian makes it impossible to assign individual lines in the experimental spectra to theoretical transitions. Therefore, to conduct a detailed analysis, it is necessary to simulate the spectra in their entirety with the aid of a large computer.

We have written a computer program to calculate the line positions and intensities determined from the theoretical expressions given in Sec. III. This program determines the line positions to an accuracy of 0.1 G. An iterative procedure was included to recalculate the line positions until the value of H used in the higher-order hyperfine terms of Eq. (3) was within 1 G of the final line position.

Then, a Gaussian distribution was assumed for each line, and the first derivatives of the resultant theoretical spectra were plotted on a digital plotter.

The first derivative peak-to-peak linewidth of the Gaussian distribution was taken initially as 2.3 G, the average linewidth of the experimental lines (Figs. 1–3). Values for the various spin-Hamiltonian constants used in the preliminary computations, except for a, were also obtained approximately from the observed spectra. The g value (~ 2.00) and A (~ 100 G) were estimated from the ESR spectrum of the CaF$_2$ sample containing 1 wt% Mn^{2+} which showed only six broad ^{55}Mn hyperfine lines.

The initial values of the superhyperfine tensor components $T_\parallel$ and $T_\perp$ can be estimated from the observed superhyperfine structure associated with the $m = \frac{1}{2}$ hyperfine component based on the assumptions that (i) the fine structure is collapsed for this component and (ii) the $\Delta k_i = 0$ superhyperfine transitions are dominant. To determine these superhyperfine constants, it is necessary to measure the superhyperfine splitting for α_i equal to 90° and 0°. These two splittings can be obtained from the spectra with $\vec{H} \parallel [110]$ and $\vec{H} \parallel [111]$. As can be seen from Table I, the eight nn fluorines fall into essentially two groups for each of these orientations of $\vec{H}$, and the superhyperfine lines from each group of fluorines overlap to reduce the total number of lines observable in both cases. This situation is similar to that for the atomic hydrogen center in CaF$_2$ investigated by Hall and Schumacher.[15] Following their example, we estimated $T_\parallel \cong 15.4$ G and $T_\perp \cong 6.4$ G.

The fine-structure constant a cannot be estimated directly from the experimental spectra since the fine-structure splitting is not clearly distinguishable. Furthermore, an estimate of a is not possible from the near collapse of the fine structure for the $m = \frac{1}{2}$ hyperfine component in the manner of Baker, Bleaney, and Hayes[1] since, theoretically, no single value of a can collapse the fine structure for $m = \frac{1}{2}$ in all three crystallographic directions because of the angular dependence of the cubic crystal field [Eq. (2)]. However, in the initial stages of analysis, an attempt was made to simulate the experimental spectra with small values of a without the third-order term of Eq. (3). Although the values of all the spin-Hamiltonian parameters were widely varied, no value of a produced theoretical spectra that fit the experimental data.

However, when the third-order hyperfine term of Eq. (3) was included, a convincing visual fit to the experimental spectrum was achieved with $a = 0$. Based on this theoretical spectrum, the best-fit set of spin-Hamiltonian parameters was obtained by the following procedure. The experimental spectrum was digitized point by point with an average

interval between points of 0.3 G. (Care was taken to ensure that all inflection points were included and a linear interpolation to 0.1 G was made by the computer between the measured points.) A theoretical spectrum was then calculated for sets of parameters (including the linewidth) about the preliminary values, and the difference in intensity between the theoretical and experimental spectra was squared and accumulated for the entire range of the spectrum in steps of 0.1 G. The minimum of the accumulated difference was then used as a criterion to find the best-fit parameters for the spin Hamiltonian. The resultant values are

$$g = 2.0010 \pm 0.0005 \ ,$$

$$A = -100.8 \pm 0.1 \ \text{G} \ ,$$

$$a = 0 \pm 0.1 \ \text{G} \ , \tag{10}$$

$$T_\perp = +6.3 \pm 0.1 \ \text{G} \ ,$$

$$T_\parallel = +15.3 \pm 0.1 \ \text{G} \ .$$

The best-fit theoretical spectra along the three major crystallographic directions are depicted with the experimental spectra in Figs. 1–3. The best-fit linewidth determined by the computer program was 2.1 G. Values outside the indicated limits produce poorer visual and calculated fits to the experimental spectra. Although smaller error limits are indicated quantitatively by the computer program, they cannot be used with confidence since the program does not perform a true least-squares analysis.

V. DISCUSSION

Considering the complexity involved in the experimental spectra and the many theoretical ESR transitions possible for the Mn^{2+} center, the agreement between the experimental data and theoretical spectra displayed in Figs. 1–3 is excellent. For all three major crystallographic axes investigated, the theoretical spectra consistently yield the important details of the observed fluorine superhyperfine structure, including the weak lines barely observable above the experimental noise level. Using the values of the spin-Hamiltonian constants obtained from the fit of the X-band experimental spectra, K_a-band theoretical spectra were also calculated. As in the case of the X-band work, the resultant theoretical spectra agree extremely well with our K_a-band ESR data.

There appears to be, however, a minor discrepancy between the theoretical and experimental spectra in the resolution of the fluorine superhyperfine structure. For example, note that with $\vec{H} \parallel [100]$, the theoretical superhyperfine structure associated with the $m = \frac{3}{2}$ ^{55}Mn hyperfine component exhibits better resolution than the corresponding experimental superhyperfine structure; on the

other hand, the experimental superhyperfine structure for $m = \frac{5}{2}$ is somewhat better resolved than the $m = \frac{5}{2}$ theoretical superhyperfine structure.

An attempt has been made to determine the reason for this discrepancy. As a result of our extensive computer simulation of the experimental spectra with a wide range of the spin-Hamiltonian constants, we do not believe that the noted discrepancy arises from an inaccurate determination of the constants of the quoted spin Hamiltonian of Eq. (1). We have also investigated other possible causes such as a small local distortion producing a very weak, axially symmetric crystalline field, as well as high-order Zeeman terms. However, inclusion of these effects in the spin Hamiltonian did not yield any apparent improvement.

One conceivable reason for the discrepancy in resolution may arise from the use of the same linewidth for all of the ESR transitions in computing the theoretical spectra, whereas the actual linewidth may be slightly different for different transitions because of possible variations in the spin-Hamiltonian constants from one Mn^{2+} site to another. In addition, it is possible that the neglected higher-order ^{55}Mn hyperfine terms may also be a contributing factor to the observed discrepancy. However, in view of the excellent over-all fitting already achieved both at X and K_a bands, and because the inclusion of these effects in the theoretical spectra would require a complete restructuring of the computer calculation, we have not further pursued the investigation of these possibilities.

One of the significant results of the present work is that the cubic crystal field splitting a of the Mn^{2+} center is found to be zero within 0.1 G. During the computer analysis of the experimental data, particular attention was devoted to determining the value of a as accurately as possible. We have found that it is not possible to achieve a better theoretical fit to the experimental spectra with values of a outside of $a = 0 \pm 0.1$ G.

Another interesting result is the surprising importance of the third-order ^{55}Mn hyperfine term even though A is only -100.8 G. This third-order term has been neglected in the past as being too small, but it has a critical influence on the appearance of the over-all spectra. In fact, the reason for the relative simplicity of the fluorine superhyperfine structure for the $m = \frac{1}{2}$ ^{55}Mn hyperfine component is the near cancellation of the second- and third-order hyperfine terms, rather than cancellation of the second-order hyperfine term with a small cubic field splitting as has been widely accepted in the past.

It should also be pointed out that as a result of the present analysis, the absolute signs of the fluorine superhyperfine interaction constants $T_{\parallel}$ and $T_{\perp}$ have been unambiguously determined for $CaF_2 : Mn^{2+}$. As can be seen in Eq. (4), the fluorine superhyperfine interaction depends on the electronic magnetic quantum number M. Thus, if an ESR center possesses $S \geq 1$ and undergoes a substantially large crystal-field splitting such that the resultant fine structure is well resolved and distinguishable in the experimental spectra, the superhyperfine structure would be different for the different fine-structure components. [12] This would enable one to determine the signs of the superhyperfine constants (relative to the crystal-field term) by carefully investigating the details of the experimental superhyperfine structure for various fine-structure component lines.

Since the cubic crystal-field splitting a was found to be zero, one might consider it impossible to determine the signs of the superhyperfine constants for the Mn^{2+} center from the ESR data alone. However, one should note the following facts: As already mentioned in Sec. III, the high-order ^{55}Mn hyperfine terms cause each of the six hyperfine component lines to be split into five lines corresponding to the various $M - 1 - M$ electronic transitions, since the higher-order terms depend on M [see Eq. (3)]. For a given ^{55}Mn hyperfine component (for example, the highest field component), the actual assignment of the five lines to the various $M - 1 - M$ transitions becomes reversed with respect to the magnetic field if the sign of the hyperfine coupling constant A is reversed. [16] This situation corresponds exactly to that caused by the reversal of the sign of the crystal-field constant for the case of a finite crystal-field splitting and negligible higher-order hyperfine terms with a given sign of A; i.e., for the purpose of determining the sign of $T_{\parallel}$ and $T_{\perp}$, the high-order hyperfine terms behave in a manner similar to a crystal-field splitting.

It can be seen therefore that the details of the fluorine superhyperfine structure for the Mn^{2+} center would depend on the relative signs of $T_{\parallel}$ and $T_{\perp}$ with respect to that of A. Indeed, we have found that the theoretical spectra exhibit a fluorine superhyperfine structure completely different from that shown in Figs. 1–3 when the signs of $T_{\perp}$ and $T_{\parallel}$ are changed. Since the absolute sign of A has been determined for $CaF_2 : Mn^{2+}$ by the low-temperature experiment (see Sec. II), we have been able to determine unambiguously the absolute signs of $T_{\parallel}$ and $T_{\perp}$ for the fluorine superhyperfine interaction.

VI. CONCLUSIONS

The complex experimental ESR spectra of the Mn^{2+} center in the CaF_2 lattice have been successfully explained in a quantitative manner. As a result of this investigation, the various ambiguities associated with previous investigations have been removed, and a correct understanding of this ESR

center has been achieved.

It is expected that the ESR spectra from the other fluoride crystals (SrF_2, BaF_2, and CdF_2) can be analyzed with the same degree of accuracy as that obtained for the CaF_2 : Mn^{2+} system. It would be interesting to compare the various spin-Hamiltonian parameters, particularly those of the fluorine superhyperfine interactions, in an effort to investi-

gate the detailed electronic structure of the manganese-fluorine complex MnF_8 for the various hosts.

†This research was conducted under the McDonnell Douglas Independent Research and Development Program.

*Consultant, McDonnell Douglas Research Laboratories. Permanent address: Department of Physics, St. Louis University, St. Louis, Missouri 63103.

[1]J. M. Baker, B. Bleaney, and W. Hayes, Proc. Roy. Soc. (London) 247A, 141 (1958).

[2]T. P. P. Hall, W. Hayes, and F. I. B. Williams, Proc. Phys. Soc. (London) 78, 883 (1961).

[3]J. E. Drumheller, J. Chem. Phys. 38, 970 (1963).

[4]V. M. Vinokurov and V. G. Stepanov, Fiz. Tverd. Tela 6, 380 (1964) [Sov. Phys. Solid State 6, 303 (1964)].

[5]M. G. Mier, J. Chem. Phys. 51, 4011 (1969).

[6]U. Ranon and D. N. Stamires, Chem. Phys. Letters 2, 286 (1968).

[7]G. G. P. Van Gorkom, J. Phys. Chem. Solids 31,

905 (1969).

[8]R. Lacroix, Helv. Phys. Acta 30, 374 (1957).

[9]R. J. Richardson, Sook Lee, and T. J. Menne, Phys. Rev. B 2, 2295 (1970).

[10]L. M. Materrese and C. Kikuchi, J. Phys. Chem. Solids 1, 117 (1956).

[11]B. Bleaney, Phil. Mag. 42, 441 (1951).

[12]A. M. Clogston, J. P. Jaccarino, M. Peters, and L. R. Walker, Phys. Rev. 117, 1222 (1960).

[13]U. Ranon and J. S. Hyde, Phys. Rev. 141, 259 (1966).

[14]It turns out that for Mn^{2+} in CaF_2 the ratio of total intensities of the allowed and forbidden transitions is roughly 9 : 1.

[15]J. L. Hall and R. T. Schumacher, Phys. Rev. 127, 1892 (1962).

[16]This is clearly illustrated in Fig. 1 of Ref. 9.

Temperature Dependence of Optical Absorption Lines from Iron Atoms in a Krypton Matrix*

H. Micklitz† and P. H. Barrett

Department of Physics, University of California, Santa Barbara, California 93106

(Received 26 June 1971)

The optical absorption spectrum of iron atoms isolated in a krypton matrix contains two narrow lines at $\lambda = 3004 \pm 0.5$ and 2969 ± 1.0 Å. These lines are related to the two multiplet lines $3d^6 4s\ ^5D_4 - 3d^7 (a\ ^4F) 4p\ ^5D_4°$ and $3d^6 4s^2\ ^5D_4 - 3d^7 (a\ ^4F) 4p\ ^5D_3°$. The linewidths (full width at half-maximum) at a matrix temperature of 4 K are 42 ± 1.5 and 38 ± 4 cm^{-1}, respectively. The lines are asymmetric (high-energy tail) and the linewidths increase with increasing temperature. From the line-shape analysis of the 3004 Å line at 4.2 and 20.5 K, the effective Debye temperature of solid krypton as probed by iron atoms is determined: The temperature dependence of linewidth yields $\Theta_D = 60 \pm 5$ K; the asymmetry of the line gives $\Theta_D = 53 \pm 6$ K.

Rare-gas matrix-isolated atoms have been studied in the last 20 years by optical absorption[1] and emission[2-4] spectroscopy. Until recently these studies have been confined to alkali-metal atoms or other metal atoms with total symmetric (S-state) ground states. Mann and Broida[1] have extended the optical absorption experiments to rare-gas matrix-isolated transition-metal atoms.

In most calculations made to account for the observed matrix-induced energy shifts of the absorption and emission lines from impurity atoms in rare-gas matrices (e.g., McCarthy and Robinson,[5] Brith and Schnepp,[6] Micklitz[7]), the interaction of the

impurity atom with lattice motions has been neglected, i.e., the rare-gas solid has been treated as a static nondeformable lattice.

Zwanzig[8] has developed expressions for emission and absorption line shifts and for linewidths by using the same assumptions as McCarthy and Robinson[5] but with the additional consideration of the influence of lattice vibrations on the mean positions and widths of the lines. This analysis is a straightforward application of a theory developed by Lax[9] who calculated the shape of optical absorption and emission lines of impurity atoms in crystals with emphasis on the role of lattice vibrations. Lax shows,